Fatigue Crack Growth Prediction by the Non-local Critical Plane Model

Z. Mróz[1], A. Seweryn[2] and A. Tomczyk[2]

[1] Institute of Fundamental Technological Research, Polish Academy of Sciences, Świętokrzyska 21, 00-049 Warsaw, Poland, zmroz@ippt.gov.pl
[2] Białystok University of Technology, Faculty of Mechanical Engineering, Wiejska 45 C, 15-351 Białystok, Poland, seweryn@pb.bialystok.pl

ABSTRACT. *The present paper is concerned with modelling of fatigue crack initiation and propagation by applying the non-local critical plane model, proposed by Seweryn and Mróz [1,2]. Using the linear elastic stress field at the front of crack or sharp notch the damage growth on a physical plane is specified in terms of mean values of stress and strength function. When the damage zone reaches a critical length, crack growth accompanies damage evolution. The model is applied to study crack propagation under cyclically varying tension-compression and predictions are compared with experimental data.*

INTRODUCTION

Most engineering components subjected to variable loads experience multiaxial stress and strain states for which principal stress vary in time. Usually the components contain stress concentrators (notches, holes, joints), which amplify nominal stresses and generate fatigue cracks. In most cases of combined loads the notch tip stress and strain fields do not vary proportionally and multiaxial fatigue parameters should be introduced to provide crack initiation and propagation conditions. Most fatigue data in the form of *S–N* curves have been generated for uniform specimens under uniaxial loading and next used to predict fatigue life for notched specimens in terms of local stress and strain amplitudes.

The proposed multiaxial fatigue theories can be divided in several categories, namely stress-based, strain-based or energy-based models, critical plane criteria and cohesive crack models. Let us refer to the uniaxial cyclic loading for which the *S–N* curve is usually specified by the relation

$$\frac{\Delta\varepsilon}{2} = \frac{\sigma_{\mathrm{f}}'}{E}\left(2N_{\mathrm{f}}\right)^{b} + \varepsilon_{\mathrm{f}}'\left(2N_{\mathrm{f}}\right)^{c}, \tag{1}$$

where $\Delta\varepsilon$ denotes the strain amplitude, $\varepsilon_{\mathrm{f}}'$ is the uniaxial fatigue ductility component, σ_{f}' denotes the uniaxial fatigue strength coefficient, c and b are ductility and strength parameters, finally N_{f} denotes the critical number of cycles corresponding to crack initiation. The uniaxial criterion (1) can be generalized to multiaxial stress and strain states

by introducing effective stress and strains expressed in terms of scalar invariants.The uniaxial strain amplitude can now be replaced by the deviatoric effective strain or energy effective strain amplitude and applied to predict crack initiation from Eq. (1). For high cycle fatigue when only elastic strains occur the use of effective stress or strain can provide good correlation of uniaxial data with multiaxial stress states.
For low cycle fatigue the account should be made for plastic dissipation. The use of cyclic plastic work as a damage parameter has been recommended, cf. Morrow [3], Garud [4] and others. Assuming the decomposition of strain increment into elastic and plastic parts, we have that the accumulated plastic work can be related to the fatigue life:

$$\Delta W_{\mathrm{c}}^{\mathrm{p}} = A N_{\mathrm{f}}^{\alpha}, \tag{2}$$

where A and α are the fatigue parameters. It must be remembered, however, that the computation of multiaxial plastic work requires fairly sophisticated models of cyclic plasticity. To generate a representative fatigue parameter for both low and high-cycle regimes, the elastic and plastic strain energies can be combined as it was proposed by Ellyin and Gołoś (5).

The *critical plane* approaches have been widely used in correlating fatigue data and in formulating fatigue conditions. This approach is natural since plane crack initiation and growth is dependent on the surface traction components and the resulting crack opening and shear provide damage strains associated with the crack surface.

Consider a physical plane in the material element specified by a unit normal vector $\mathbf{n}$. The plane traction vector and its components are

$$\mathbf{T} = \sigma\,\mathbf{n}, \quad \boldsymbol{\sigma}_{\mathbf{n}} = (\mathbf{n}\cdot\boldsymbol{\sigma}\,\mathbf{n})\mathbf{n}, \qquad \boldsymbol{\tau}_{\mathbf{n}} = (\mathbf{I}-\mathbf{n}\otimes\mathbf{n})\boldsymbol{\sigma}\,\mathbf{n}\,. \tag{3}$$

Similarly, the surface strain components are

$$\boldsymbol{\Gamma} = \boldsymbol{\varepsilon}\,\mathbf{n}, \quad \boldsymbol{\varepsilon}_{\mathbf{n}} = (\mathbf{n}\cdot\boldsymbol{\varepsilon}\,\mathbf{n})\mathbf{n}, \qquad \boldsymbol{\gamma}_{\mathbf{n}} = (\mathbf{I}-\mathbf{n}\otimes\mathbf{n})\boldsymbol{\varepsilon}\,\mathbf{n}\,, \tag{4}$$

where $\mathbf{I}$ is the unit tensor. The critical plane can be assumed in advance as *representative plane* on which the critical condition is satisfied. It was first Findley et al. [6] who postulated that the representative plane is the maximum shear plane with both shear strain and normal strain amplitudes specifying the damage parameter, thus

$$\gamma_{\mathrm{c}}^{*} = \frac{\Delta\gamma_n}{2} + k\frac{\Delta\varepsilon_n}{2}, \tag{5}$$

where k is the weighting factor. A particular form of this condition was proposed by Brown and Miller [7]. McDiarmid [8] provided an alternative stress condition expressing the fatigue parameter in terms of shear and normal stress amplitudes on the maximal shear planes. Other criteria of this type combine the shear strain amplitude and the maximal normal stress acting on the maximal shear plane, cf. Socie [9].

These conditions can be easily applied to the case of proportional loading. However, for non-proportional loading, the proper definition of stress and strain amplitudes should be generated. Furthermore, experimental observations indicate that cracks do not

develop on maximum shear planes for all metals. For instance, for 304 stainless steel the critical plane corresponds to maximal tensile strain and usually the plane orientation depends on the type of loading.

A more consistent approach is obtained by not specifying the critical plane approach in advance but requiring the maximum of the failure condition to be reached with respect to all orientations, thus

$$\max_{(\mathbf{n})} F(\sigma_n, \tau_n, \varepsilon_n, \gamma_n) = F_{\mathrm{c}}^*, \tag{6}$$

where F_{c} represents the critical value reached by the failure condition. The present definition provides the critical plane which is also the *extremal plane*, so that the critical condition is not violated on other potential failure planes.

A particular form of Eq. (6) is obtained by applying the strain energy density associated with the amplitudes of stress and strain components acting on the critical plane, cf. Glinka et al. [11]

$$W_{\mathrm{c}}^* = \max_{(\mathbf{n})} \left[\frac{\Delta\gamma_n}{2} \frac{\Delta\tau_n}{2} + \frac{\Delta\varepsilon_n}{2} \frac{\Delta\sigma_n}{2} \right]. \tag{7}$$

This parameter represents only a fraction of the strain energy. However, it does not account for the effect of mean stress. An alternative energy condition was proposed by Chu [10] by combining maximum normal and shear stresses with the strain amplitudes, thus

$$W_{\mathrm{c}}^* = \max_{(\mathbf{n})} \left(2\tau_n^{\max} \Delta\gamma_n + \sigma_n^{\max} \Delta\varepsilon_n \right). \tag{8}$$

The cohesive crack model pioneered by Dugdale [12] and Barrenblatt [13] can be regarded as further extension of the critical plane approach. It is assumed that when the critical stress or strain condition is reached on the *extremal* plane, the gradual separation on this plane is developed, thus generating a damage zone preceding the crack. The critical stress condition can be assumed in the form

$$\max_{\mathbf{n}} F[\sigma_n, \tau_n, \sigma_{\mathrm{c}}(\delta)] \le 0, \tag{9}$$

where $\sigma_{\mathrm{c}}(\delta)$ is the cohesive strength value. The displacement discontinuity on the critical plane

$$\boldsymbol{\delta} = \mathbf{u}^+ - \mathbf{u}^- = [\mathbf{u}], \qquad \boldsymbol{\delta} = \boldsymbol{\delta}_n + \boldsymbol{\delta}_t, \tag{10}$$

is then associated with the critical stress condition (9), for instance, by the associated flow rule

$$\dot{\delta}_n = \dot{\lambda} \frac{\partial F_{\mathrm{c}}}{\partial \sigma_n}, \qquad \dot{\delta}_t = \dot{\lambda} \frac{\partial F_{\mathrm{c}}}{\partial \tau_n}, \qquad \dot{\lambda} > 0, \tag{11}$$

where multiplier $\dot{\lambda}$ can be specified from the consistency condition of (9), $\dot{F}=0$, and δ is a scalar measure of displacement discontinuity. Assuming the critical stress value to decrease with δ, a full decohesion, $\sigma_c = 0$, occurs at $\delta = \delta_c$. The cohesive crack model predicts the generation and growth of the damage zone governed by the cohesive law $\sigma_c = \sigma_c(\delta)$ and also growth of crack occurring at $\delta = \delta_c$. The application of the cohesive crack model to study growth of fatigue crack was presented by de Andrés et al. [14].

The concept of *non-local* description of crack initiation and propagation is natural when a heterogeneous material structure is considered with randomly varying stress and strain. The non-local values on any physical plane can be specified as follows

$$\bar{\sigma}_n(\mathbf{x}) = \frac{1}{S_r}\int \alpha_r|\mathbf{x}-\mathbf{y}|\sigma_n(y)\mathrm{d}S_y, \qquad \bar{\tau}_n(\mathbf{x}) = \frac{1}{S_r}\int \alpha_r|\mathbf{x}-\mathbf{y}|\tau_n(y)\mathrm{d}S_y, \tag{12}$$

where S_r represents the averaging area and $\alpha_r(r)$, $r=|\mathbf{x}-\mathbf{y}|$, is the weighting function which decreases with the distance r from the point $\mathbf{x}$. The simplest case is when $\alpha_r = 1$ within the specified domain of size α_r and vanishes outside. Then Eq. (14) provide the mean values of stresses within specified plane domains.

The formulation of Seweryn and Mróz [1, 2] followed the idea of non-local stress or strain measures on the critical plane area of size $d_0 \times d_0$. Denoting the resulting shear stress in the plane by τ_n, so that

$$\tau_n = \|\boldsymbol{\tau}\| = \left(\tau_{n1}{}^2 + \tau_{n2}{}^2\right)^{\frac{1}{2}} \tag{13}$$

The local failure function takes the form

$$R_{f\sigma} = R_\sigma\left(\frac{\sigma_n}{\sigma_c}, \frac{\tau_n}{\tau_c}\right), \tag{14}$$

where σ_c and τ_c are the failure stresses in tension and shear. Analogously to the analysis of the strength of cracked body considering the microcrack opening and contact with accompanying slip and friction cf. Mróz and Seweryn [15], the elliptic condition for $\sigma_n \geq |\tau_n|\tan\varphi_d$ and the Coulomb condition for $\sigma_n < |\tau_n|\tan\varphi_d$ was assumed (Fig. 1), thus

$$R_\sigma = \begin{cases} \left[\left(\dfrac{\sigma_n}{\sigma_c}\right)^2 + \left(\dfrac{\tau_n}{\tau_{cA}}\right)^2\right]^{0,5}, & \sigma_n \geq |\tau_n|\tan\varphi_d \\ \dfrac{1}{\tau_c}\left[|\tau_n| + \sigma_n \tan(\varphi_f + \varphi_d)\right], & \sigma_n < |\tau_n|\tan\varphi_d \end{cases} \tag{15}$$

where φ_d and φ_f denotes the dilatancy angle and the friction angle respectively.

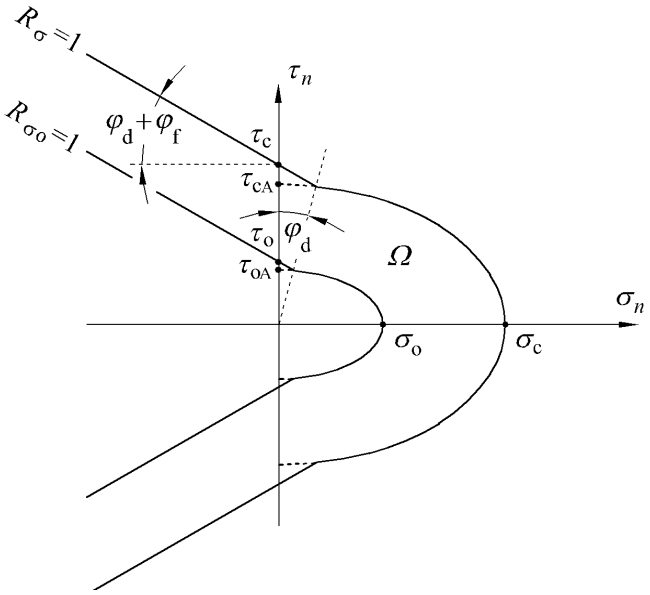

Figure 1. Damage initiation and failure curves in (σ_n, τ_n) plane: elliptic condition for $\sigma_n \geq |\tau_n| \tan\varphi_d$ and the Coulomb condition for $\sigma_n < |\tau_n| \tan\varphi_d$.

The non-local failure function can now be expressed as follows [16]

$$R_{f\sigma} = \max_{(\mathbf{n},\mathbf{x_0})} \overline{R}_\sigma = \max_{(\mathbf{n},\mathbf{x_0})} \left[\frac{1}{{d_0}^2} \int_0^{d_0} \int_0^{d_0} R_\sigma \, d\xi_1 d\xi_2 \right] \tag{16}$$

and the failure condition is

$$R_{f\sigma} - 1 = 0. \tag{17}$$

For the case of cyclic fatigue condition, the threshold surface of damage initiation was assumed in a similar form to Eq. (14), namely

$$\max_{(\mathbf{n},\mathbf{x_0})} R_{\sigma o}\left(\frac{\sigma_n}{\sigma_o}, \frac{\tau_n}{\tau_o} \right) - 1 = 0 \tag{18}$$

and the non-local condition of damage initiation is

$$R_{f\sigma o} - 1 = \max_{(\mathbf{n},\mathbf{x_0})} \left[\frac{1}{{d_0}^2} \int_0^{d_0} \int_0^{d_0} R_{\sigma o}\left(\frac{\sigma_n}{\sigma_o}, \frac{\tau_n}{\tau_o} \right) d\xi_1 d\xi_2 \right] - 1 = 0 \tag{19}$$

where for simplicity it is assumed that $R_o = R_{\sigma o}/R_\sigma$.

The damage growth for stress states lying within the domain bounded by the failure surface $R_{f\sigma} = 1$ and the damage initiation surface $R_{f\sigma o} = 1$ is specified by the damage evolution rule

$$\mathrm{d}\omega_n = A_\sigma \left(\frac{R_\sigma - R_o}{1 - R_o} \right)^n \frac{\mathrm{d}\hat{R}_\sigma}{1 - R_o}, \tag{20}$$

where A and n are material parameters. The effective failure function increment $\mathrm{d}\hat{R}_\sigma$ is specified by the following relation

$$\mathrm{d}\hat{R}_\sigma = \begin{cases} \mathrm{d}R_\sigma^* & \text{for } \mathrm{d}R_\sigma^* > 0 \text{ and } R_\sigma > R_o \\ 0 & \text{for } \mathrm{d}R_\sigma^* \le 0 \text{ or } R_\sigma \le R_o \end{cases} \tag{21}$$

and

$$\mathrm{d}R_\sigma^* = \frac{\partial R_\sigma}{\partial \sigma_n}\mathrm{d}\sigma_n + \frac{\partial R_\sigma}{\partial \tau_n}\mathrm{d}\tau_n \tag{22}$$

An alternative specification of increment $\mathrm{d}\hat{R}_\sigma$ can be expressed in the following form

$$\mathrm{d}\hat{R}_\sigma = \frac{\partial R_\sigma}{\partial \sigma_n}\mathrm{d}\hat{\sigma}_n + \frac{\partial R_\sigma}{\partial \tau_{n1}}\mathrm{d}\hat{\tau}_{n1} + \frac{\partial R_\sigma}{\partial \tau_{n2}}\mathrm{d}\hat{\tau}_{n2} \tag{23}$$

where effective stress increments (for $R_\sigma > R_o$) are specified by the relations

$$\begin{aligned} \mathrm{d}\hat{\sigma}_n &= \mathrm{d}\sigma_n \quad \text{for} \quad \mathrm{d}\sigma_n \ge 0 \text{ and } \sigma_n \ge 0 \\ \mathrm{d}\hat{\sigma}_n &= 0 \quad \text{for} \quad \mathrm{d}\sigma_n < 0 \text{ and } \sigma_n < 0 \end{aligned} \tag{24}$$

and

$$\begin{aligned} \mathrm{d}\hat{\tau}_{ni} &= \mathrm{d}\tau_{ni} \quad \text{for} \quad \tau_{ni}\mathrm{d}\tau_{ni} \ge 0 \\ \mathrm{d}\hat{\tau}_n &= 0 \quad \text{for} \quad \tau_{ni}\mathrm{d}\tau_{ni} < 0 \end{aligned} \tag{25}$$

The damage parameter is assumed to affect both σ_c, τ_c, so that

$$\sigma_c(\omega) = \sigma_c^*(1 - \omega_n)^p, \qquad \tau_c(\omega) = \tau_c^*(1 - \omega_n)^p \tag{26}$$

where σ_c^* and τ_c^* are failure stresses in tension and shear for the undamaged material, p is material parameter.

The present model is conceptually similar to the cohesive crack model, as the existence of damage zone preceding the crack front is assumed. However, the analysis is fully based on linear elastic stress distribution and no decohesive displacement is

assumed. The model was applied to simulate damage accumulation in tubular elements under combined cyclic flexure and torsion, cf. Seweryn and Mróz [2], or fatigue crack initiation in plane elements with sharp notches under tension and shear cf. Molski and Seweryn [17].

Now, we shall discuss application of this model to simulation of fatigue crack propagation in uniaxial and multiaxial loading conditions.

FATIGUE CRACK PROPAGATION IN UNIAXIAL LOADING

To illustrate the model applicability, consider a plate of uniform thickness (Fig. 2a) with the edge crack of length l, loaded by a cyclically varying stress σ of amplitude $\Delta\sigma$ and mean value $\sigma_m = \Delta\sigma/2$. The material is assumed to be linear elastic, but exhibiting a process or damage zone Ω of length d_0 at the crack tip (Fig. 2b).

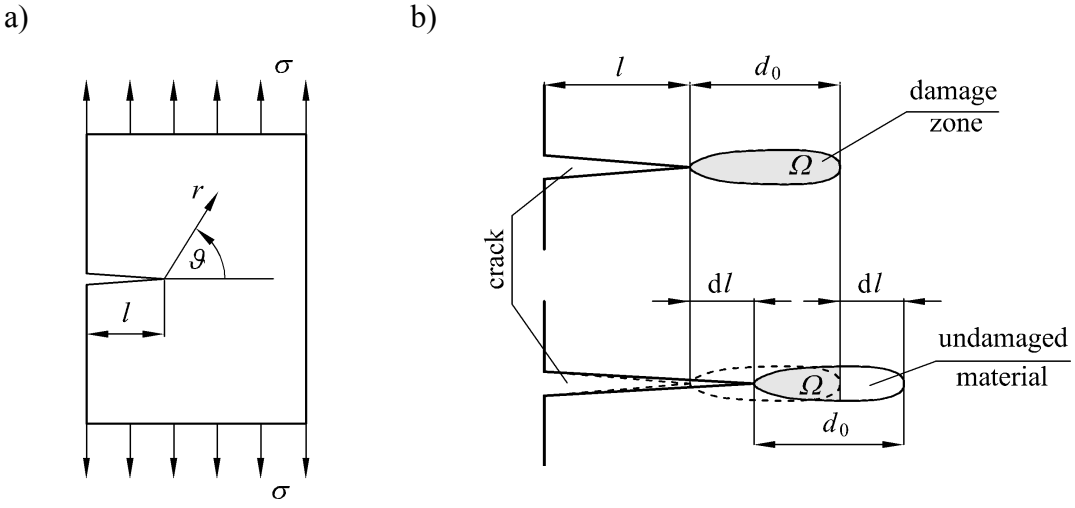

Figure 2. a) Plate with the edge crack, b) scheme of the damage zone propagation.

The existence of the localized damage zone is usually assumed for the cohesive crack model with an additional rule relating stress to displacement discontinuity. Here, however, the stress distribution will be treated within the linear elasticity but the existence of a process zone will be accounted for using the non-local damage rule discussed in the previous section.

It is assumed that damage growth occurs only in the damage zone and is specified by the mean value $\overline{\omega}_n$ affecting the critical stress σ_c. The mean value of the normal stress in the zone Ω equals

$$\overline{\sigma}_n = \frac{1}{d_0}\int_0^{d_0} \sigma_n \mathrm{d}r = \frac{2K_\mathrm{I}}{\sqrt{2\pi d_0}}, \tag{27}$$

where K_I is the stress intensity factor for mode I. Let us note that $\overline{\sigma}_n$ is twice as large as the stress value at the end of damage zone.

The cycle of fatigue loading we divide into four stages (Fig. 3).

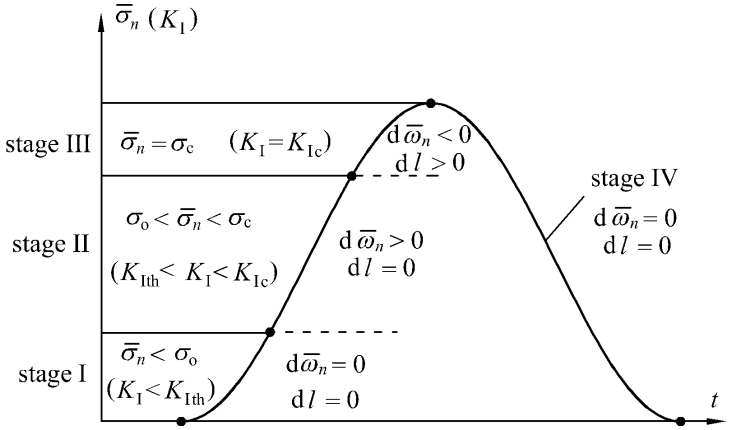

Figure 3. Consecutive stages in one loading cycle.

When the stress in a cycle increases from zero, in the stage I there is no damage growth as $\overline{\sigma}_n < \sigma_\mathrm{o}$ and $K_\mathrm{I} < K_\mathrm{Ith}$ where σ_o and K_Ith are the damage initiation threshold values. Let us note that both σ_o and K_Ith depend on the damage state, thus

$$\sigma_\mathrm{o} = \sigma_\mathrm{o}^*(1-\overline{\omega}_n)^p, \qquad K_\mathrm{Ith} = K_\mathrm{Ith}^*(1-\overline{\omega}_n)^p \tag{28}$$

where σ_o^* and K_Ith^* are the respective values for the undamaged material.

In the second stage $\sigma_\mathrm{o} < \overline{\sigma}_n < \sigma_\mathrm{c}$, the damage growth occurs in the zone Ω, according to the following rule

$$\mathrm{d}\overline{\omega}_n = A\left(\frac{\overline{\sigma}_n - \sigma_\mathrm{o}}{\sigma_\mathrm{c} - \sigma_\mathrm{o}}\right)^n \frac{\mathrm{d}\overline{\sigma}_n}{\sigma_\mathrm{c}^* - \sigma_\mathrm{o}^*}, \qquad \mathrm{d}\overline{\sigma}_n > 0, \qquad \overline{\sigma}_n > \sigma_\mathrm{o}, \tag{29}$$

and we have

$$\sigma_\mathrm{c} = \sigma_\mathrm{c}^*(1-\overline{\omega}_n)^p, \qquad K_\mathrm{Ic} = K_\mathrm{Ic}^*(1-\overline{\omega}_n)^p \tag{30}$$

where σ_c^* and K_Ic^* are the critical values for the undamaged material.

Let us note that in Eq. (29) the stress difference $\left(\sigma_\mathrm{c}^* - \sigma_\mathrm{o}^*\right)$ in the denominator occurs.

This differs from the original formulation of Seweryn and Mróz [1] where the form $(\sigma_c - \sigma_o)$ was used. Introduce the ratio $\sigma_o^*/\sigma_c^* = \eta$ and assume that

$$\eta = \frac{\sigma_o^*}{\sigma_c^*} = \frac{\sigma_o}{\sigma_c} = \frac{K_{Ith}}{K_{Ic}} = \frac{K_{Ith}^*}{K_{Ic}^*}. \tag{31}$$

In view of Eqs (14), (28) and (30), the damage evolution rule takes the form

$$\mathrm{d}\overline{\omega}_n = \frac{A}{(1-\eta)^{n+1}}\left(\frac{K_I}{K_{Ic}^*(1-\overline{\omega}_n)^p} - \eta\right)^n \frac{\mathrm{d}K_I}{K_{Ic}^*}. \tag{32}$$

In this stage the stress value $\overline{\sigma}_n$ increases but the values of σ_o and σ_c decrease, according to Eqs (28) and (30). When $\overline{\sigma}_n$ reaches the critical value $\overline{\sigma}_n = \sigma_c$ and $K_I = K_{Ic}$, the crack growth process occurs, so that the condition

$$\begin{aligned} & F_c = \overline{\sigma}_n - \sigma_c = \overline{\sigma}_n - \sigma_c^*(1-\overline{\omega}_n)^p = 0 \\ \text{or} \qquad & \overline{F}_c = K_I - K_{Ic} = K_I - K_{Ic}^*(1-\overline{\omega}_n)^p = 0 \end{aligned}, \qquad \mathrm{d}l > 0 \tag{33}$$

is satisfied.

The consistency condition for the growth crack is

$$\mathrm{d}F_c = \mathrm{d}\overline{\sigma}_n - \mathrm{d}\sigma_c = 0, \qquad \mathrm{d}\overline{F} =_c \mathrm{d}K_I - \mathrm{d}K_{Ic}(\overline{\omega}_n) = 0. \tag{34}$$

We have therefore

$$\frac{2K_I}{\sqrt{2\pi d_0}} - \sigma_c^*(1-\overline{\omega}_n)^p = 0 \qquad \text{or} \qquad \frac{2\mathrm{d}K_I}{\sqrt{2\pi d_0}} + p\sigma_c^*(1-\overline{\omega}_n)^{p-1}\mathrm{d}\overline{\omega}_n = 0. \tag{35}$$

Let us note that $K_I = K_I(\sigma, l)$, so we have

$$\mathrm{d}K_I = \frac{\partial K_I}{\partial \sigma}\mathrm{d}\sigma + \frac{\partial K_I}{\partial l}\mathrm{d}l\,. \tag{36}$$

In most cases the first term dominates as the crack growth value $\mathrm{d}l/\mathrm{d}N$ is small. Then

$$\mathrm{d}K_I \cong M_k\sqrt{\pi l}\,\mathrm{d}\sigma \tag{37}$$

where M_k depends on the geometry of the plate.

The damage growth during the propagation stage is decomposed into two terms

$$\mathrm{d}\overline{\omega}_n = \mathrm{d}\overline{\omega}_{n1} + \mathrm{d}\overline{\omega}_{n2}, \qquad \mathrm{d}\overline{\omega}_{n1} > 0, \qquad \mathrm{d}\overline{\omega}_{n2} < 0 \tag{38}$$

where the first term is associated with loading increment and the second is associated with damage zone propagation so:

$$\mathrm{d}\overline{\omega}_n = \frac{2A\mathrm{d}K_\mathrm{I}}{\sqrt{2\pi d_0}\left(\sigma_\mathrm{c}^* - \sigma_\mathrm{o}^*\right)} - \overline{\omega}_n \frac{\mathrm{d}l}{d_0} \qquad \text{or} \qquad \frac{\mathrm{d}l}{d_0} = -\left[1 + \frac{pA}{(1-\eta)}(1-\overline{\omega}_n)^{p-1}\right]\frac{\mathrm{d}\overline{\omega}_n}{\overline{\omega}_n}. \quad (39)$$

Integrating Eq. (39), we obtain

$$\frac{\Delta l}{d_0} = -\int_{\overline{\omega}_{n\mathrm{k}}}^{\overline{\omega}_{n\mathrm{p}}} \left[1 + \frac{pA}{(1-\eta)}(1-\overline{\omega}_n)^{p-1}\right]\frac{\mathrm{d}\overline{\omega}_n}{\overline{\omega}_n}. \quad (40)$$

where $\overline{\omega}_{n\mathrm{k}}$ and $\overline{\omega}_{n\mathrm{p}}$ denote the damage values at the beginning and the end of the propagation stage III.

The relation (40) specifies the crack growth during one cycle, so that $\Delta l = \mathrm{d}l/\mathrm{d}N$. The consecutive stage IV corresponds to elastic unloading, so that

$$\mathrm{d}\overline{\sigma}_n < 0 \quad (\mathrm{d}K_\mathrm{I} < 0), \qquad \mathrm{d}\overline{\omega}_n = 0, \qquad \mathrm{d}l = 0. \quad (41)$$

Using the double logarithmic scale, the crack propagation curves are shown in Figs 4a and 4b, for varying exponent values n and for varying values of damage growth parameter A. The curves can be compared with the usual diagrams $\mathrm{d}l/\mathrm{d}N = \mathrm{f}(\Delta K_\mathrm{I})$ available in literature. It is seen that the crack propagation curves correspond qualitatively well to experimental curves. When K_I tends to K_Ic^*, the crack propagation rate tends to infinity, when K_I tends to K_Ith, the propagation rate tends to zero (or the logarithmic measure to minus infinity).

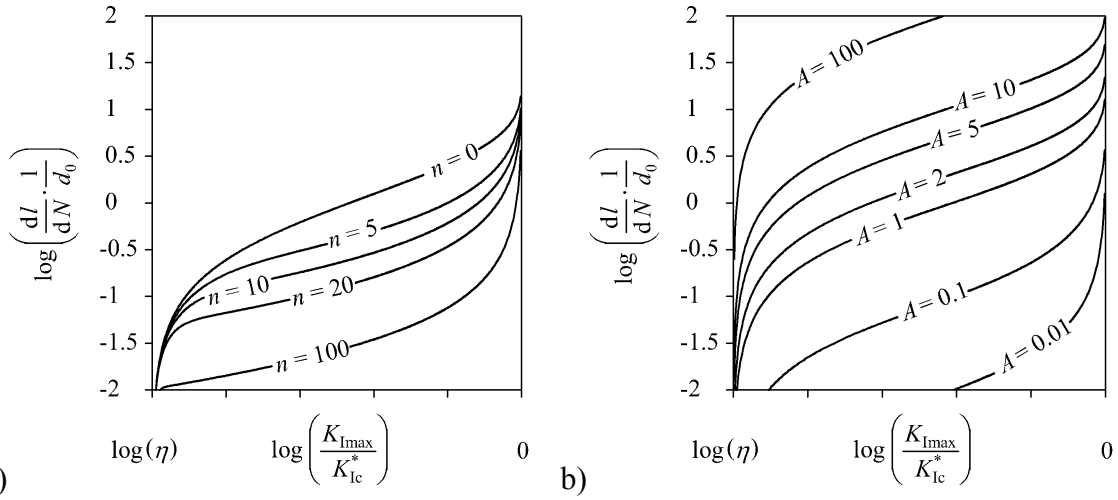

Figure 4. Crack propagation curves $\log(\Delta l/d_0)$ versus $\log\left(K_\mathrm{Imax}/K_\mathrm{Ic}^*\right)$: a) dependence on the exponent n, b) dependence on the parameter A.

Figures 5a and 5b illustrate the effect of overloading on subsequent crack propagation rate for single overloading cycle and different values of A.

Let us note that when K_{I} tends to K_{Ic}^{*} (or $\overline{\sigma}_n$ tends to σ_{c}^{*}), then the case of brittle fracture occurs. Let us remind that the first term of Eq. (36) dominates for stable crack growth, and the second term is greater for the unstable growth. To formulate brittle fracture condition, we can disregard the first term of Eq. (36) because

$$\frac{\partial K_{\mathrm{I}}}{\partial \sigma}\mathrm{d}\sigma << \frac{\partial K_{\mathrm{I}}}{\partial l}\mathrm{d}l \qquad \text{so} \qquad \mathrm{d}K_{\mathrm{I}} \approx \frac{\partial K_{\mathrm{I}}}{\partial l}\mathrm{d}l. \tag{42}$$

It is justified in the case of load control (then $\mathrm{d}\sigma/\mathrm{d}l \geq 0$). When kinematic control occurs, we have $\mathrm{d}\sigma/\mathrm{d}l < 0$ and it is necessary to consider the complete form of (49).

Rearranging Eq. (35) we can formulate the brittle fracture criterion in the following form:

- crack propagation condition:

$$K_{\mathrm{I}} = K_{\mathrm{Ic}}^{*}\left(1-\overline{\omega}_n\right)^{p} \tag{43}$$

- unstable crack growth condition:

$$\frac{\partial K_{\mathrm{I}}}{\partial l} \geq \frac{pK_{\mathrm{Ic}}^{*}\left(1-\overline{\omega}_n\right)^{p}\overline{\omega}_n}{d_0\left[1-\overline{\omega}_n+\dfrac{pA}{(1-\eta)}\left(1-\overline{\omega}_n\right)^{p}\right]}. \tag{44}$$

Figure 6 shows the graphic illustration of these equations.

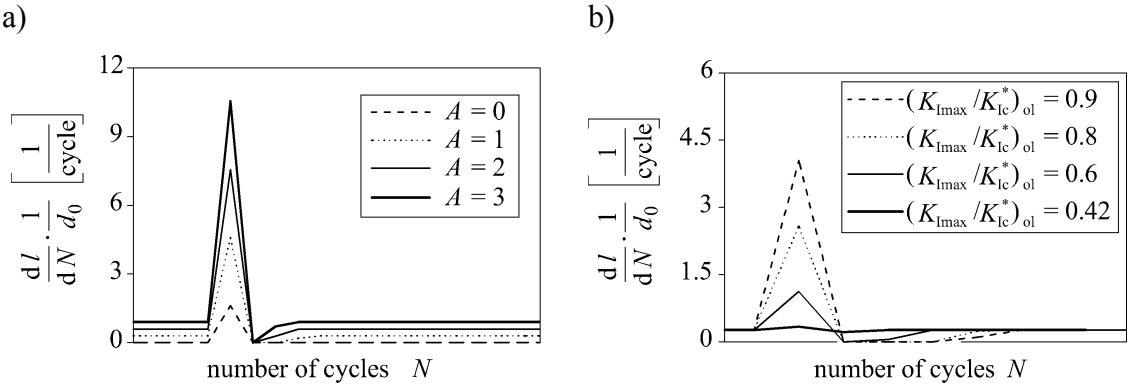

Figure 5. The effect of a single overloading cycle on crack propagation rates: a) single overloading cycle $K_{\mathrm{Imax}}/K_{\mathrm{Ic}}^{*} = 0.9$ and subsequent cycles $K_{\mathrm{Imax}}/K_{\mathrm{Ic}}^{*} = 0.5$, b) single overloading cycle $K_{\mathrm{Imax}}/K_{\mathrm{Ic}}^{*} = 0.42$, $K_{\mathrm{Imax}}/K_{\mathrm{Ic}}^{*} = 0.6$ $K_{\mathrm{Imax}}/K_{\mathrm{Ic}}^{*} = 0.8$ and $K_{\mathrm{Imax}}/K_{\mathrm{Ic}}^{*} = 0.9$ with subsequent cycles $K_{\mathrm{Imax}}/K_{\mathrm{Ic}}^{*} = 0.4$.

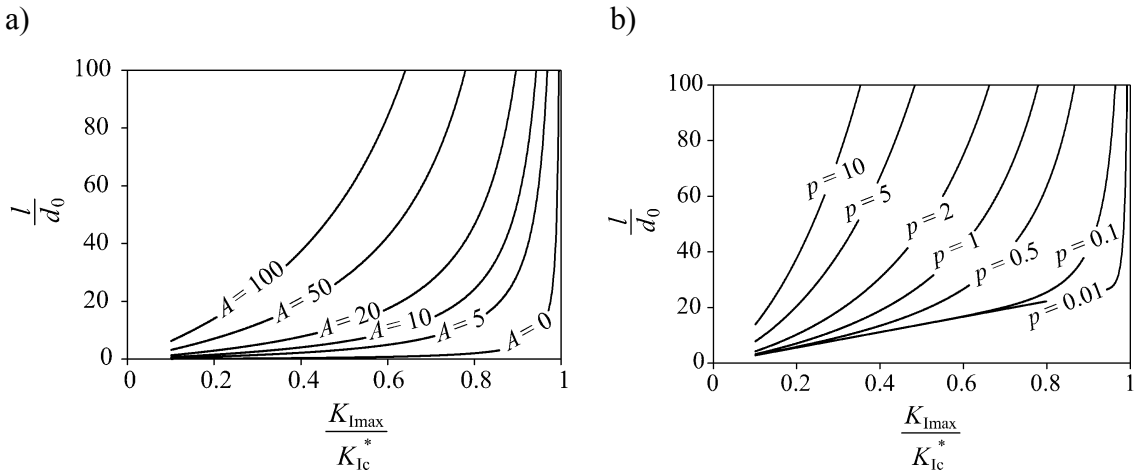

Figure 6. Dependence of the critical crack length on K_{I} value for unstable crack growth a) $p = 1$, $\eta = 0.1$, b) $A = 50$, $\eta = 0.1$.

The model presented at the beginning of this chapter considers the translation of the damage zone at the propagating crack tip. It is possible to propose an alternative approach considering both: motion of the damage zone and growth of this zone. So, let us make an assumption that damage growth zone Ω exists at the tension crack tip. The length of this zone is r_0. It is assumed that normal stress and damage are specified, respectively, by the mean values $\overline{\sigma}_n$ and $\overline{\omega}_n$.

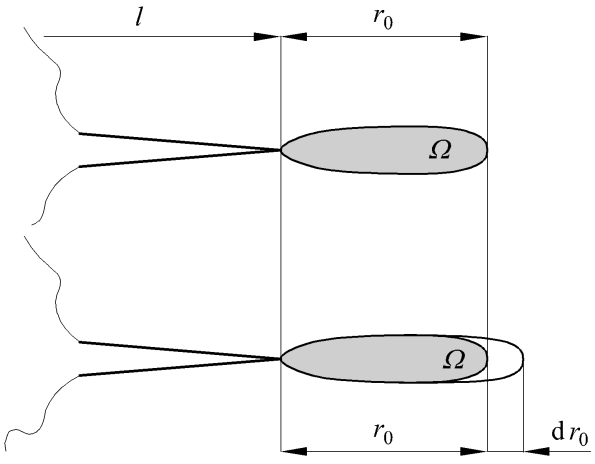

Figure 7. Damage zone growth scheme.

The actual value r_0 can be evaluated from the equation

$$\frac{1}{r_0}\int_0^{r_0}\left(\max_t \frac{\sigma_{\vartheta\vartheta}(t)}{\sigma_{\mathrm{c}}(t)}\right)\mathrm{d}r = \max_t \frac{\overline{\sigma}_n(t)}{\sigma_{\mathrm{c}}(t)} = 1, \qquad r_0 \le d_0, \tag{45}$$

where t denotes time. The critical value of σ_{c} depends on the damage state in view of Eq. (30). In Eq. (45) we have to place the maximal value of ratio $\overline{\sigma}_n / \sigma_{\mathrm{c}}$ during a fatigue loading process. Considering asymptotic solution for stress fields (first, singular term only), we can rewrite Eq. (45) in the form as follows

$$r_0 = \frac{2}{\pi\left(\sigma_{\mathrm{c}}^*\right)^2}\max_t\left[\frac{K_{\mathrm{I}}(t)}{\left(1-\overline{\omega}_n(t)\right)^p}\right]^2. \tag{46}$$

Let us consider uniaxial cyclic loading. Now we divide the cycle of fatigue loading into five stages (Fig. 8).

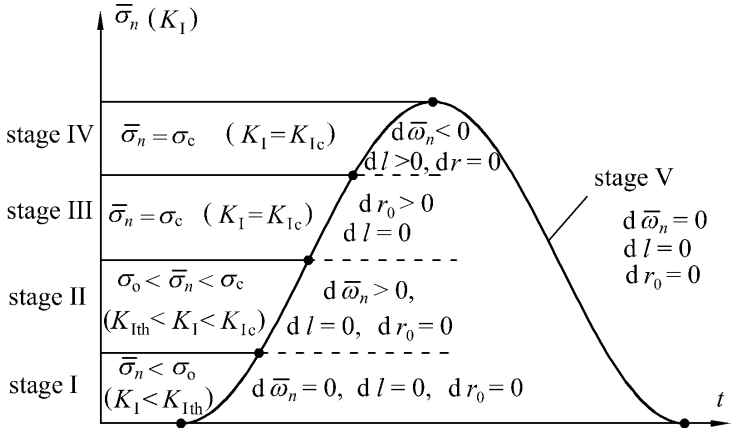

Figure 8. Five stages of loading in one cycle.

In the first stage, the mean value $\overline{\sigma}_n$ is lower than the damage initiation threshold value σ_{o}, thus

$$\overline{\sigma}_n = \frac{1}{r_0}\int_0^{r_0}\sigma_{\vartheta\vartheta}(\vartheta = 0)\mathrm{d}r < \sigma_{\mathrm{o}}\,, \tag{47}$$

where σ_{o} depends on the damage state, see Eq. (40).
In stage I (Fig. 8) there is no damage growth, damage zone growth and crack propagation, so we have

$$\mathrm{d}\overline{\omega}_n = 0, \qquad \mathrm{d}r_0 = 0, \qquad \mathrm{d}l = 0. \tag{48}$$

When the stress value $\overline{\sigma}_n$ reaches the threshold value σ_{o}, the damage growth process occurs, but the zone length and crack length remain unchanged (stage II of cycle), thus

$$\mathrm{d}\overline{\omega}_n > 0, \qquad \mathrm{d}r_0 = 0, \qquad \mathrm{d}l = 0. \tag{49}$$

This stage is the same as the stage II in the approach presented earlier, so $\overline{\sigma}_n < \sigma_{\mathrm{c}}$. The damage growth rule is defined by Eq. (29), the values σ_{o} and σ_{c} decrease according to Eq. (30).

When the stress value $\overline{\sigma}_n$ reaches the critical value σ_{c} damage zone growth process occurs (stage III of cycle), so

$$\overline{\sigma}_n = \sigma_{\mathrm{c}}^*\left(1-\overline{\omega}_n\right)^p, \qquad \mathrm{d}r_0 > 0, \qquad \mathrm{d}l = 0. \tag{50}$$

Except for the stress equality condition, the stable damage zone growth condition (47) must be satisfied. The damage growth $\mathrm{d}\overline{\omega}_n$ depends on stress variation in zone Ω and zone length growth with the terms $\left(\mathrm{d}\overline{\omega}_{n1}\right)$ and $\left(\mathrm{d}\overline{\omega}_{n2}\right)$ according to Eq. (38). The condition (35b) takes the form

$$\mathrm{d}\sigma_n\left[1+\frac{pA}{(1-\eta)}\left(1-\omega_n\right)^{p-1}\right] = \omega_n\left(1-\omega_n\right)^{p-1} p\sigma_{\mathrm{c}}^*\frac{\mathrm{d}r_0}{r_0}. \tag{51}$$

The increment of the mean value $\overline{\sigma}_n$ depends on load increase (stress intensity factor increase) and damage zone growth, thus

$$\mathrm{d}\overline{\sigma}_n = \frac{1}{\sqrt{2\pi r_0}}\left(2\mathrm{d}K_{\mathrm{I}} - K_{\mathrm{I}}\frac{\mathrm{d}r_0}{r_0}\right) \tag{52}$$

Combining Eqs (51) and (52) we obtain

$$\begin{aligned} 2\mathrm{d}K_{\mathrm{I}}\left[1+\frac{pA}{(1-\eta)}\left(1-\omega_n\right)^{p-1}\right] &= K_{\mathrm{I}}\frac{\mathrm{d}r_0}{r_0}\left[1+\frac{pA}{(1-\eta)}\left(1-\omega_n\right)^{p-1}\right] + \\ &+ \omega_n\left(1-\omega_n\right)^{p-1} p\sigma_{\mathrm{c}}^*\sqrt{2\pi}\frac{\mathrm{d}r_0}{\sqrt{r_0}}. \end{aligned} \tag{53}$$

When the size r_0 reaches the critical value d_0, the crack propagation process occurs (stage IV of cycle). The crack propagation criterion takes the form

$$r_0 = d_0, \qquad \mathrm{d}\overline{\sigma}_n > 0 \tag{54}$$

In this stage the mean value $\overline{\sigma}_n$ equals the critical value σ_c (like in stage III) and the damage zone size remains unchanged, so that

$$\overline{\sigma}_n = \sigma_c, \qquad \mathrm{d}r_0 = 0, \qquad \mathrm{d}l > 0 \tag{55}$$

and the stable crack growth condition is (34).

The analysis of crack propagation condition and stable crack growth condition is presented at the beginning of this chapter. In stage V we have

$$\mathrm{d}\overline{\sigma}_n < 0, \qquad \mathrm{d}\overline{\omega}_n = 0, \qquad \mathrm{d}r_0 = 0, \qquad \mathrm{d}l = 0, \tag{56}$$

and the unloading process occurs.

EXPERIMENTAL VERIFICATION

The experimental program was executed by testing plane specimens of PMMA with edge notches (Fig. 9).

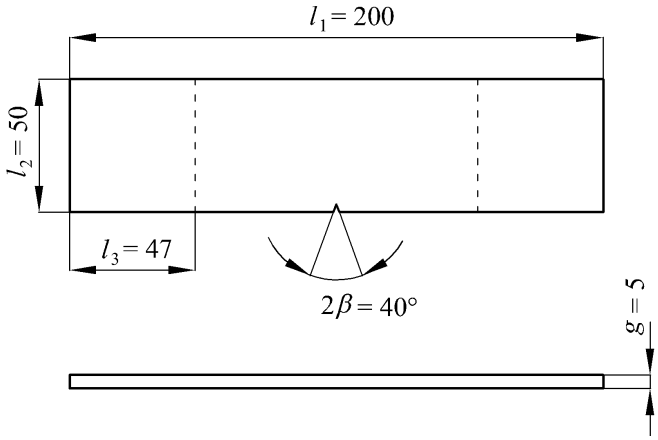

Figure 9. Plane specimens with wedge shaped notches of the angle $2\beta = 40°$.

The material selection was motivated by its linear elastic response and the possibility of visual observation of crack tip. The test were carried out using MTS tensile machine and the crack growth measurement was executed by means of the spiral microscope (VEB Carl Zeiss Jena) with the accuracy of order of 0.001 mm. Figure 10 presents the cracked specimens and Figures 11 and 12 present the experimental data of crack growth measurement and the present model prediction. The comparison with prediction of Paris model

$$\frac{\mathrm{d}l}{\mathrm{d}N} = C\left(\Delta K\right)^m \tag{57}$$

was also presented.

a) b)

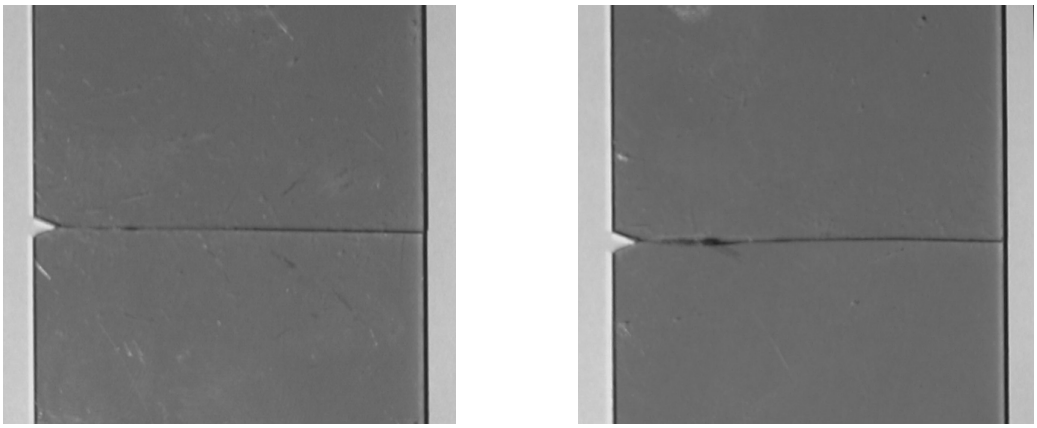

Figure 10. Photographs of cracked samples: a) sample *12A*, b) sample *14B*.

Five types of specimens were used (*12A*, *12B*, *12C*, *14A*, *14B*) in tests. The parameter specification for the Paris model is presented in Table 1 and of the present model in Table 2.

Table 1. Parameter specification for Paris model.

No of sample	C	m
12A	6.19×10^{-7}	3.31
12B	7.09×10^{-7}	3.55
12C	6.65×10^{-7}	3.78
14A	1.52×10^{-6}	5.21
14B	8.66×10^{-7}	4.43

Table 2. Parameter specification for present model.

No of sample	A	n	p	$K^*_{\mathrm{Ith}}\ [\mathrm{MPa}\sqrt{\mathrm{m}}]$	$K^*_{\mathrm{Ic}}\ [\mathrm{MPa}\sqrt{\mathrm{m}}]$	d_0 [mm]
12A	0.009	9	1	0.5	1.2	0.16
12B	0.013	12.5		0.6	1.2	
12C	0.007	7		0.55	1.2	
14A	0.024	7		0.6	1.35	
14B	0.017	8		0.6	1.35	

It is seen that there is a scatter of parameter values, typical for fatigue tests for PMMA. The present model predicts much better fatigue crack growth, especially for high values of K_{Imax} close to K_{Ic}^{*}. We note that the value of parameter p equals one, and the following relations are valid:

$$\begin{aligned} \sigma_{\mathrm{o}} &= \sigma_{\mathrm{o}}^{*}(1-\overline{\omega}_n), & \tau_{\mathrm{o}} &= \tau_{\mathrm{o}}^{*}(1-\overline{\omega}_n), \\ \sigma_{\mathrm{c}} &= \sigma_{\mathrm{c}}^{*}(1-\overline{\omega}_n), & \tau_{\mathrm{c}} &= \tau_{\mathrm{c}}^{*}(1-\overline{\omega}_n) \end{aligned} \tag{58}$$

The specification of damage zone growth is then essentially simplified, cf. Eq. (57). It is also interesting to note that the maximum size of damage zone $d_0 = 0.16$ mm was confirmed from both static and cyclic loading tests, providing good correlation with experimental data.

a)

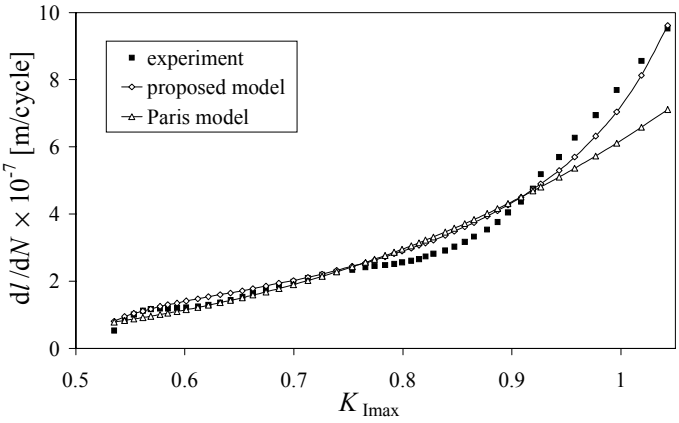

b)

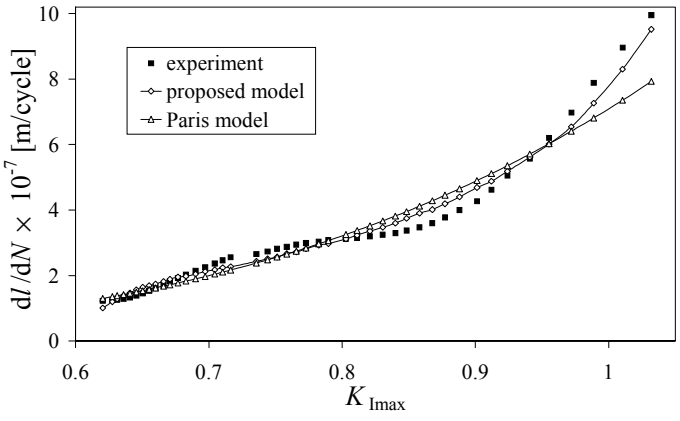

c)

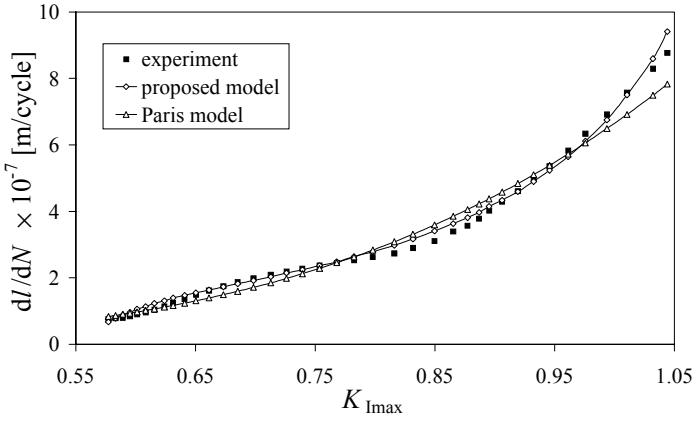

Figure 11. Diagrams of fatigue crack growth: comparison of experimental data with model prediction: a) specimen *12A*, b) specimen *12B*, c) specimen *12C*.

a)

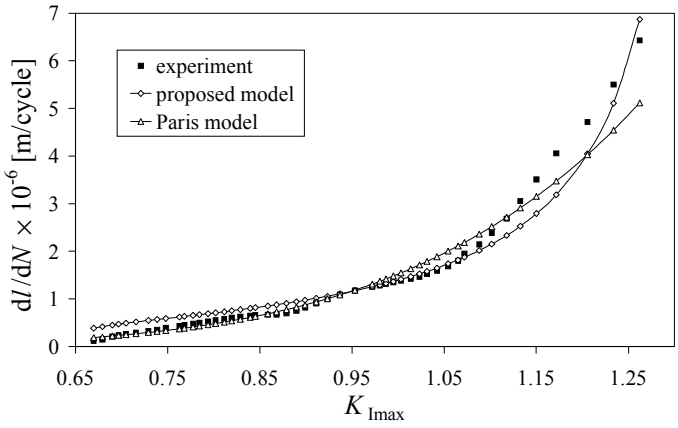

b)

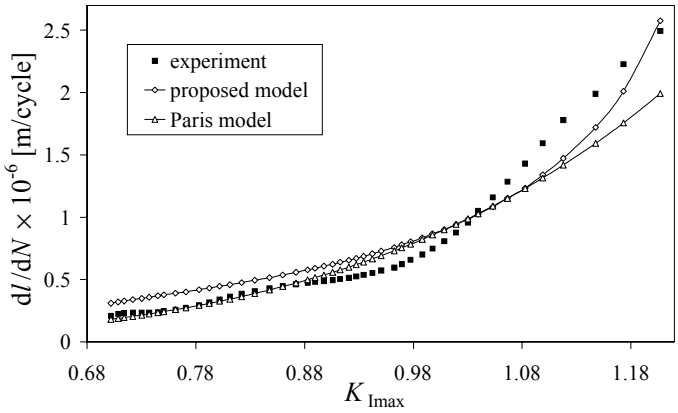

Figure 12. Diagrams of fatigue crack growth: comparison of experimental data with model prediction: a) specimen *14A*, b) specimen *14B*.

The biaxial stress programs are actually tested and the prediction of crack paths will be compared with measurement.

CONCLUDING REMARKS

The present paper provides the model of analysis of crack initiation and propagation for monotonic and variable loading. The damage zone of varying length and tending to a limit value was introduced with the averaged measures of stress and damage within the zone. The zone is assumed to propagate with the crack tip when the critical propagation condition is reached. The stable and unstable growth stages can be treated.

The model proposed enables calculation of crack growth in the linear elastic material, analysis of the effect of overloads on crack growth rate and specification of crack path for arbitrary biaxial non-proportional loading. The analysis was referred to asymptotic stress fields near the crack tip. However, it can be extended to more complex descriptions containing more terms of asymptotic expansions or generated by the approximate methods. The analysis can also be extended to three dimensional stress states and the associated damage zones. The model assumptions are similar to those of the cohesive crack model where the damage zone opening displacement provides the dissipation mechanism due to crack growth, and the length of damage zone is related to the specific dissipation energy. Here the size of the damage zone is an essential parameter affecting the rate of growth.

REFERENCES

1. Seweryn A., Mróz Z. (1996) In: *Multiaxial Fatigue and Design*, pp. 259-280, Pineau A., Cailletaud G., Lindley T.C. (Eds), Mech. Eng. Publ., London.
2. Seweryn A., Mróz Z. (1998) *Int. J. Solids Struct.* **35**, 1599-1616.
3. Morrow J. (1965) In: *Internal Friction Damping and Cyclic Plasticity*, pp. 45-87, ASTM STP 378.
4. Garud Y.S. (1981) *Engng Mat. Tech.* **103**, ASME, 118-125.
5. Gołoś K., Ellin F. (1988): *Journ. Pressure Vessel Techn.* **1**, 36-44.
6. Findley W. N., Coleman J. J. and Handley B. C. (1956) In: *Proc. Int. Conf. Fatigue of Metals*, The Inst. Mech. Eng., pp. 150-157.
7. Brown M. W., Miller K. J. (1973) A theory for fatigue failure under multiaxial stress-strain conditions, *Proc. of The Institute of Mechanical Engineers*, **187**, pp. 745-755, 1973.
8. McDiarmid D.L. (1991) *Fatigue Fract. Engng Mater. Struct.* **14**, 429-453.
9. Socie (1993) In: *Advances in Mechanical Fatigue*, pp. 7-36, ASTM STP 119
10. Chu C.C. (1995) *J. Engng Mat. Techn.* **117**, 41-49.
11. G. Glinka, G. Shen and A. Plumtree (1995) *Fatigue Fract. Eng. Mater. Struct.* **18**, 37-46.

12. Dugdale D. S. (1960): *J. Mech. Phys. Solids* **8**, 100-104.
13. Barrenblatt G.I. (1959): *J. Appl. Math. Mech.* **23**, 622-636.
14. de Andrés A., Perez J. L. and Ortiz M. (1999) *Int. J. Solids Struct.* **36**, 2231-2258.
15. Mróz Z., Seweryn A. (1998) *J. de Physique IV France* **8**, 257-268.
16. Seweryn A., Mróz Z. (1995) *Eng. Fract. Mech*. **51**, 955-973.
17. Molski K., Seweryn A. (1999) In: *Multiaxial Fatigue and Fracture*, pp. 13-24, Macha E., Będkowski W. and Łagoda T. (Eds), Mech. Eng. Publ.

ACKNOWLEDGEMENTS – The investigation described in this paper is a part of the research project No. 8 T07A 049 21 sponsored by the Polish State Committee for Scientific Research.